Structural transformations in two-dimensional transition-metal dichalcogenide MoS_2 under electron beam: insights from first-principles calculations

Kretschmer, S.; Komsa, H.-P.; Bøggild, P.; Krasheninnikov, A. V.;

Originally published:

June 2017

Journal of Physical Chemistry Letters 8(2017)13, 3061-3067

DOI: https://doi.org/10.1021/acs.jpclett.7b01177

Structural transformations in two-dimensional transition-metal dichalcogenide MoS_2 under electron beam: insights from first-principles calculations

Silvan Kretschmer,[*,†] Hannu-Pekka Komsa,[‡] Peter Bøggild,[¶] and Arkady V. Krasheninnikov[†,‡,¶]

Helmholtz-Zentrum Dresden-Rossendorf, Germany, Aalto University, Finland, and DTU Nanotech, Denmark

E-mail: s.kretschmer@hzdr.de

Abstract

The polymorphism of two-dimensional (2D) transition metal dichalcogenides (TMDs) and different electronic properties of the polymorphs make TMDs particularly promising materials in the context of the applications in electronics. Recently, local transformations from the hexagonal H to trigonal distorted T' phase in 2D MoS_2 have been induced by electron irradiation [Nat. Nanotech. 9 (2014) 391], but the mechanism of the transformations remains elusive. Using density functional theory calculations, we study the energetics of the stable and metastable phases of 2D MoS_2 when additional charge, mechanical strain and vacancies are present. We also investigate the role of finite temperatures, which appear to be critical for the

[*]To whom correspondence should be addressed
[†]Helmholtz-Zentrum Dresden-Rossendorf, Germany
[‡]Aalto University, Finland
[¶]DTU Nanotech, Denmark

transformations. Based on the results of our calculations, we propose an explanation for the beam-induced transformations which are likely promoted by charge redistribution in the monolayer due to electronic excitations combined with formation of vacancies under electron beam and build-up of the associated mechanical strain in the sample. As this mechanism should be relevant to other 2D TMDs, our results provide hints for further development and optimization of electron-beam-mediated engineering of the atomic structure and electronic properties of 2D TMDs with sub-nanometer resolution.

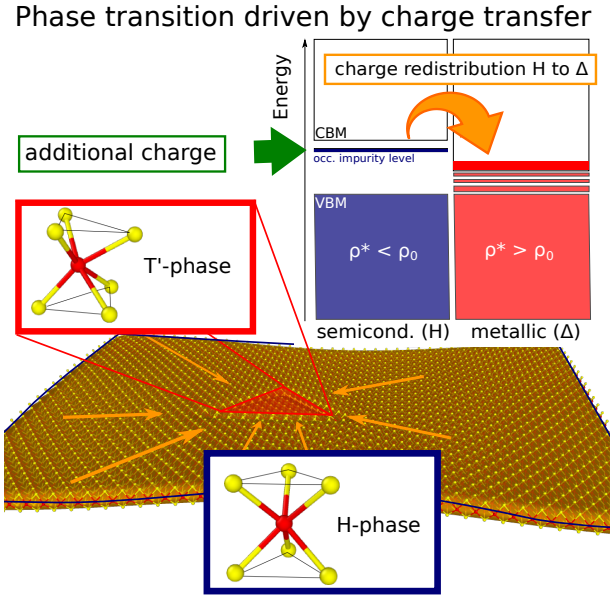

Figure 1: **TOC**

In the rapidly growing family of two-dimensional (2D) materials, monolayers of transition metal dichalcogenides (TMDs)[1,2] are of particular interest, as many of them exist as several polymorphs with drastically different electronic characteristics. Specifically, 2D TMDs can have the stable trigonal prismatic (H), octahedral (T), and distorted octahedral (T' or T") atomic configurations [1], and exhibit semiconductor, metal or topological insulator properties.[3,4] Moreover, controllable transformations from one phase to another have been reported.[5,6] Nano materials, in which

[1]Since in this work we consider monolayers only, we omit the numbers used to denote phases of the bulk TMD systems, e.g., 2H or 1T.

phase transitions associated with minute changes in the arrangement of atoms without altering material stoichiometry, not only exhibit rich physical behavior, but also open unique opportunities for the fabrication of electronic and optoelectronic devices. Indeed, metallic T' regions embedded into semiconducting H matrix in MoS_2[7] and $MoTe_2$[8] have been used as low-resistance contacts or to design MoS_2-FET transitors with sub 10 nm channel length.[9]

The energetics of the phases of various 2D TMDs and their alloys has extensively been studied by first-principles methods.[10–13] As for MoS_2, the most widely used and correspondingly explored material among 2D TMDs, ab initio calculations revealed that the pristine T phase is unstable[11] and spontaneously relaxes to T', while the metastable T' phase (T' phase is 0.55 eV higher in energy than the H phase per formula unit, f.u.) returns to H after annealing, as experimentally observed.[14,15] Normally, the transformations are mediated by strong electron doping of the system. Charge transfer upon alkaline (e.g., Li) atom intercalation leads to the transition from H to T' phase.[14,16–21] The transformation from H to T' phase has also been attributed to electron transfer from Au or Ag substrate.[22] The calculations[13,15,23–27] showed that the T' phase becomes energetically favorable over H phase when the system is strongly n-type doped, which naturally occurs under alkali metal intercalation. Calculations with Li/Na adsorption demonstrated that about 0.4 alkali atoms per f.u. are needed to induce a transition to T' phase.[25,26,28] The estimates obtained from calculations involving direct charging give a wider range of 0.08–0.8 e/f.u.[25,29] Once alkaline atoms are removed, e.g., during exfoliation to produce single sheets, the barrier between the phases is apparently high enough to preserve the metastable T' phase under ambient conditions.

At the same time, local phase transitions from the H to T phase have also been observed to occur in MoS_2 under in-situ electron beam irradiation in the transmission electron microscope (TEM).[5] Specifically, formations of triangular regions of the T phase embedded into the H matrix have been reported in MoS_2 flakes. This is a surprising result, as it is unlikely that the exposure to the electron beam of atomically thin samples in the TEM will give rise to negative charging: the other way around, the sample may acquire positive charge, especially in wide-gap semiconductors with defects, due to emission of secondary electrons,[30] as convincingly demonstrated for BN

nanotubes.[31]

Several other factors may be responsible for the phase transition. Re doping of the MoS_2 sheets was necessary to observe the transformations. Moreover, the transitions were usually initiated by the formation of extended defects ("alpha stripes") located close to Re impurities.[5] The transformed area depended exponentially on the electron dose, but not on temperature. However, temperatures above 400 °C were needed for the transformation to occur, and it is not clear what actual role the temperature played. Defects, in particular S vacancies, were produced by the electron beam in the samples, which may have played an important role, as in $MoTe_2$.[8] Vacancies in MoS_2 are known to cluster and form lines[32] giving rise to substantial strain in the atomic network, so strain should also be taken into consideration.

In this work, using first-principles calculations, we carefully study the factors that may be responsible for the transformations under electron beam as observed in Ref. 5, namely (i) mechanical strain, (ii) finite concentration of vacancies, (iii) Re impurities and local charge transfer, (iv) electronic excitations and (v) temperature. Based on the results of our analysis, we propose a possible mechanism for the phase transition from the H to T' phase in MoS_2 under electron beam. We show that while all these factors decrease the energy difference between the H and T phases, it is most likely a combination of these that gives rise to the stabilization of the metastable T' phase.

Details of calculations. To get insight into the energetics of the system, we performed density functional theory (DFT) calculations aimed at determining the energetically most favorable atomic configurations (phases) of MoS_2 and the corresponding electronic structures under different conditions. Plane wave basis set and projector augmented wave (PAW) description of the core regions were used, as implemented in the Vienna *ab initio* simulation Package (VASP) code.[33,34] The exchange and correlations were described within the Perdew-Burke-Ernzerhof (PBE) generalized gradient approximation.[35] The structure relaxations were carried out with 600 eV plane wave cutoff. The convergence criterion for forces was set to 5 meV / Å. At minimum 10 Å of vacuum perpendicular to the monolayer MoS_2 was added to avoid spurious interaction between the periodic images of the sheets. The lattice parameters of the H, T, and T' pristine phases obtained

in our calculations proved to be in a good agreement with the results of previous studies.[15,25,27,36] While the T phase was reported to appear under electron beam in Ref. 5, we found the T phase to be unstable with regard to the reconstruction to the T' phase, in accordance with Refs 15,25,27,36. We therefore concentrate on the T' phase. The DFT calculations, however, were carried out at zero temperature, while the experiments were done at 400-700 °C, and this may account for the difference in behavior. In any case, the mechanism of transformation from the H phase we propose is relevant for both T and T' phases. To account for the effects of temperature on the calculated energies, vibrational free energy was determined within harmonic approximation as implemented in the code Phonopy.[37] We employed 6×6 supercell and 2×2 k-point mesh for the H phase and 4×4 k-point mesh with Methfessel-Paxton smearing for the T' phase.

To investigate MoS_2 monolayers with different concentrations of impurities and co-existing different phases, we used super cells of different sizes. The largest supercell consisted of 20×20 unit cells corresponding to 1200 atoms. For these calculations, 300 eV plane wave cutoff and 10 meV/Å force convergence criterion were chosen. Test calculations with a cutoff of 400 eV gave essentially the same results for the energy difference between the configurations we considered. Such large supercells were necessary to include a large enough triangle-shaped metallic region into the semiconducting matrix in order to investigate charge transfer.

When comparing the energy of the phase patterned system (island of the T' phase embedded into H phase) to the reference system, the number of atoms (and electrons) need to match. However, the H/T interface is S deficient, and therefore the reference system is taken to contain a suitable S-vacancy line, since this has been found to be the lowest energy configuration for S deficient MoS_2.[32,38]

The comparison of the energetics of these two systems yielded the energetically preferable configuration for different conditions, e.g., different concentrations of Re impurities.

Effects of strain. We started our analysis by addressing the role of mechanical strain. S vacancies produced by the electron beam in MoS_2 tend to cluster and form lines,[32] which may give rise to substantial strain in the atomic network. Figure 2 presents strain defined as a difference in Mo-

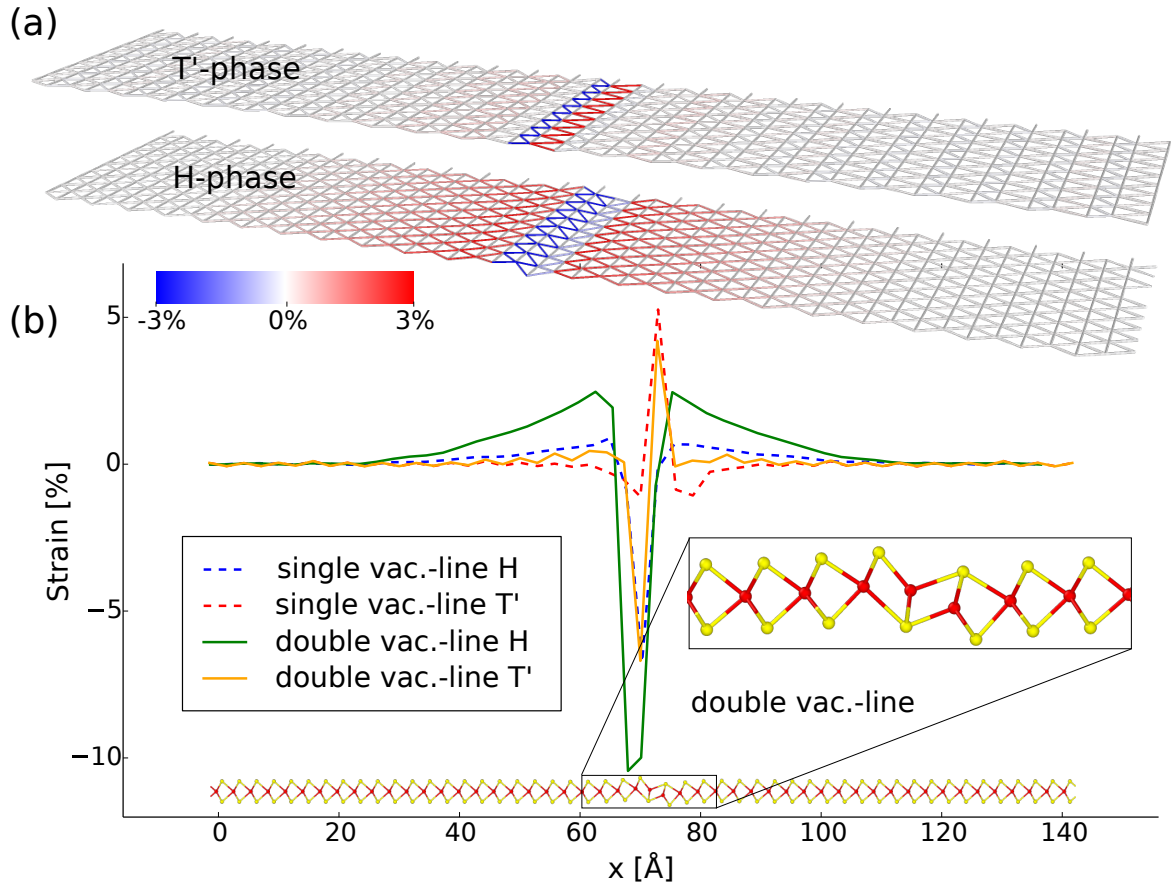

Figure 2: **Strain distribution along vacancy lines.** Line defects formed due to the coalescence of electron-beam created vacancies induce strain in 2D MoS_2. Panel (a) illustrates the strain distribution near a double vacancy line in the T' and H phases, respectively. (b) Strain along the x-axis oriented perpendicular to the vacancy line calculated for single and double vacancy lines in both phases. While vacancy lines in the T' phase give rise to local strain only, the long-ranged strain appears in the H phase.

Mo atom separation near vacancy lines in comparison to that in pristine MoS_2. It is evident that while vacancy lines in the T' phase give rise to local strain only, long-ranged strain appears in the H phase, especially near double vacancy lines: the strain distribution spreads several nanometers into the pristine region.

In order to understand how strain affects the energetics of the system, we calculated the total energy per f.u. of the H and T' phases as a function of biaxial external strain, Figure 3(a). Figure 3(b) presents the energy difference ΔE between the phases. ΔE decreases with strain, but it is evident that about 14% of strain is required to make the T' phases energetically favorable. This

value appears to be too high to be achieved in practice, especially taking into account that the experimentally measured fracture strain for MoS_2 is reported to be 6% – 11%.[39] Thus strain alone cannot explain the observed transformations.

Role of vacancies. In our analysis, we assumed that strain originates from the extended line defects which have appeared due to the agglomeration of electron-irradiation-induced vacancies. As isolated vacancies can still be present in the system, we also repeated the calculations for H and T' phases with a single vacancy concentration of 3.1%. The results of calculations are also shown in Figure 3. When vacancies are present, ΔE decreases even in the unstrained system. Similar trend was reported[8] for $MoTe_2$. As ΔE for the pristine system is much less in $MoTe_2$ (40 meV) than in MoS_2 (550 meV), only about 3% of vacancies were sufficient to make T' phase energetically favorable. Here, although vacancies decrease the energy difference between the phases, we can exclude them as the main reason for the transition from H to T' phase.

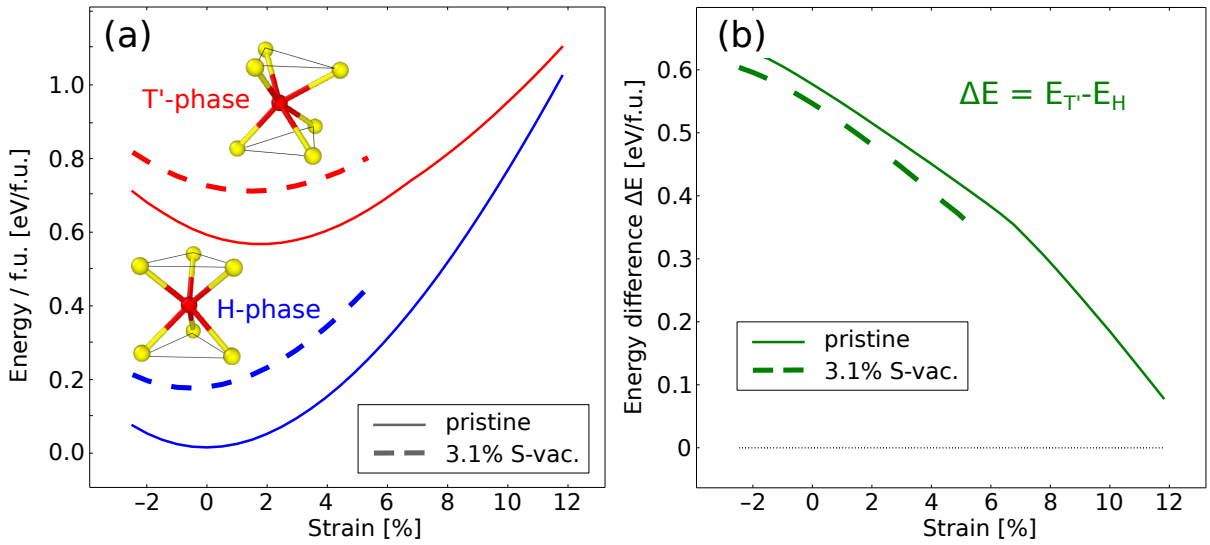

Figure 3: **Effects of mechanical strain on the energetics of the H and T' phases.** (a) Total energy per formula unit vs. biaxial strain for the semiconducting stable H phase (blue) and the metallic metastable T' phase (red). Solid lines stand for the pristine system, dashed lines for that with defects. Zero energy corresponds to the most stable H polymorph of MoS_2. (b) Energy difference between the phases $\Delta E = E_{\mathrm{T'}} - E_{\mathrm{H}}$ as a function of strain. Strain decreases ΔE, but unrealistically high values (about 14%) are required to make the T' phase energetically preferable over H phase ($\Delta E < 0$) either for the pristine system or that with vacancies.

Re impurities and local charge redistribution. So far we have considered separate phases,

tacitly assuming that the transformation happens in the whole system. No interaction or charge transfer was possible between the phases. In the experiment, however, the transformations were local, and only a small part of the system was converted to the T phase. Now we address a more realistic situation by considering a large supercell representing a T' phase triangle embedded in the H matrix, as in the experiment,[5] see Figure 4. The energy of the system with the island is compared to that of a system with single vacancy line, which has the same number of atoms. We note that the energy cost of forming an interface is small and thus it does not prevent formation of the T'-triangle. We stress that substitutional Re impurities were present in the MoS_2 flakes used in the experiment.[5] Re atom has an extra electron, as compared to Mo, so that such impurities[40] are perfect n-type dopants, giving rise to an occupied shallow state close to the conduction band minimum (CBM).[41]

At elevated temperatures these states should also result in considerable electron density at CBM. The defect states associated with vacancies are lower than those impurity states, so that partial charge redistribution is possible, as schematically shown in Figure 4. Charge redistribution, in its turn, may affect the energetics.

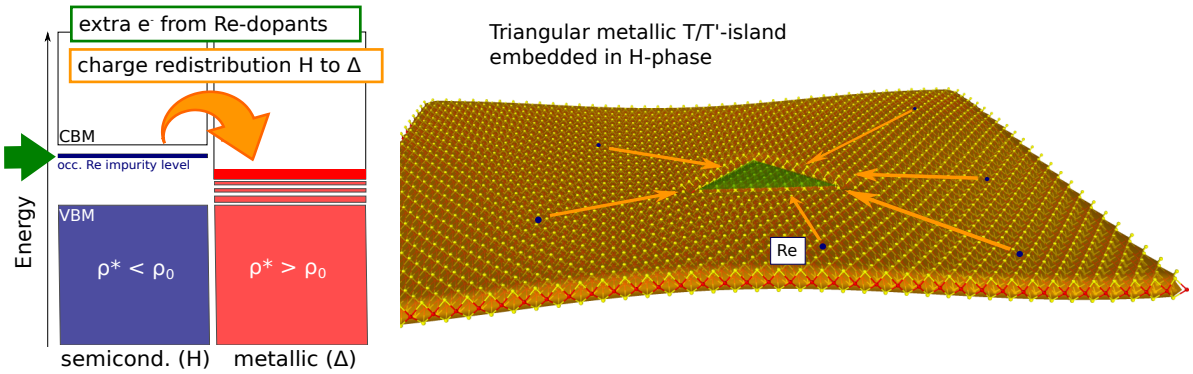

Figure 4: **Schematic representation of the charge redistribution model:** Electronic charge in the conduction band minimum originating from Re-impurities can partially go into the vacancy related states and triangle region of the metallic T' phase, so that T' phase island may get extra charge and become energetically favorable over the reference configuration with the vacancy line.

Our calculations showed that the vacancy line presented in Figure 4 has defect states in the band gap of MoS_2 which are higher in energy than the CBM of the metallic phase. To study possible

redistribution of the charge, we carried out two sets of calculations. In the first approach we added extra electrons to the supercell along with the positive background to fulfil the neutrality conditions required in the plane-wave calculations. We stress that the total energy depends on the amount of vacuum and other details of calculations in this case, and it is meaningless, as discussed previously,[42,43] but the energy difference between the two configurations is a physically valid quantity. In the second approach we substantially increased the concentration of Re impurities well above the experimental values.

Within the first approach, our calculations showed that when extra electron charge is added to the system, the energy difference between the phases (normalized to the area of the T' island) decreases, Fig. 5. The analysis of charge distribution indicates that extra electrons indeed go into the T' phase island, being localized close to its borders, as evident from the inset in Figure 5. Overall electron excess of +22% could be determined for the T'-triangle as compared to the uniform charge distribution. It is also evident, however, that considerable extra charge is required to make the T' phase energetically favorable.

In the second approach, randomly distributed (over the whole system) substitutional Re impurities were added to the systems. The calculated energy difference decreased similarly with increasing concentration of Re atoms, as evident from Figure 5. Each Re atom was expected to donate one electron. However, the necessary Re concentration to shift the energy balance towards T' phase proved to be unrealistically high, about 15%. As mentioned above, additional negative charge is not expected during the exposure of atomically thin samples to the high-energy electron beam in TEM experiments, so that although the extra negative charge should give rise to local transformation to the T' phase from the H phase with a vacancy line according to our results, this mechanism alone cannot explain the observations.

Effects of electronic excitations. The impacts of high-energy electrons onto the sample on a TEM grid give rise to core and valence electron excitations, as evident from electron energy loss spectra. Several mechanisms, including optical transitions, Auger-type processes, electron-electron and electron-phonon interactions are responsible for de-excitations. The typical times

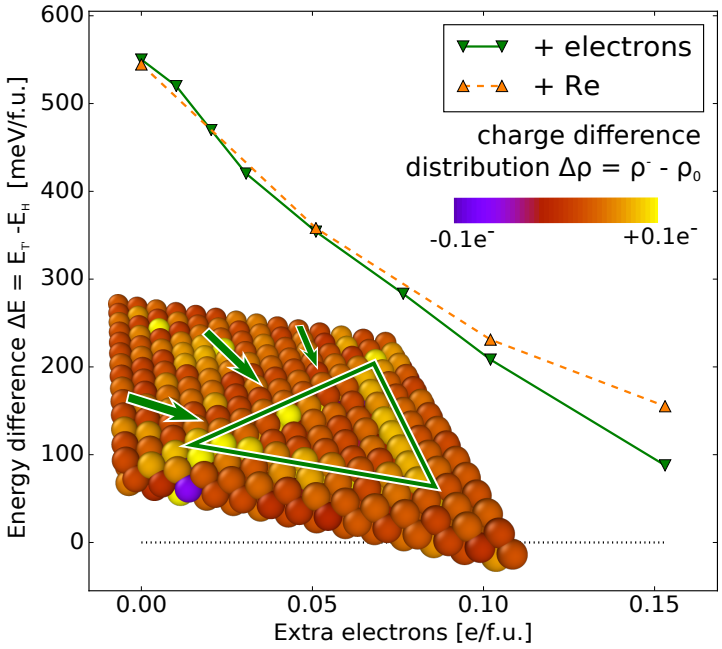

Figure 5: **Effects of local charging on the energetics of the phases.** Energy difference between the island of metallic T' phase embedded into H phase and the semiconducting reference system (H phase with a line defect). In the first computational approach we used, the number of electrons in the system is increased (solid green). In the second approach (dashed orange curve), substitutional Re impurities were introduced. The abscissa corresponds to the maximum transferable number of electrons in this case. Both curves clearly indicate that additional electrons decrease the energy difference between the systems. The inset illustrating the charge difference which corresponds to the calculation with increased electron number proves that charge transfer into the triangular metallic region (more precisely into the borders) indeed takes place. Bader analysis reveals an increase in the number of valence electrons in this region of +22% as compared to the situation with the uniformly distributed charge.

for non-radiative electron-hole recombination in the T' phase island with lateral size L should be considerably shorter than that for optical recombination in the H phase, indicating that de-excitations occur mostly in the island after the localization of the excited electrons in this area. At the same time, the non-radiative recombination time should be much larger than in bulk metallic systems due to size quantization, as in semiconductor quantum dots,[44] provided that the energy difference Δ_e between the size-qauntization-defined energy levels is larger than the optical phonon energies. This condition should be fulfilled in this case for L up to about 10 nm, as $\Delta_e \sim \hbar v_F/L$ is larger than 50 meV, characteristic optical phonon energies in MoS_2,[45] with $v_F \sim 10^6$ m/sec being

the typical Fermi velocity in metallic systems. Taking the above considerations into account, one can assume that the electronic charge associated with the electrons excited in the H phase will be localized in the T' phase area, followed by electron-hole recombinations after several electron-phonon and electron-electron scattering events, as schematically illustrated in Figure 6(a).

This may give rise to a higher electron density in the T' phase island, and as long as the sample is under the electron beam, a quasi-stationary state may develop. To investigate the energetics of the T'-island in the H matrix and the reference H system with the line defect, we carried out DFT calculations by setting zero occupancies of the states in a certain energy interval close to the valence band maximum in the combined T'-H system, and putting the corresponding electronic charge into the excited states. Such approximate approach has been previously used to describe excitation-induced semiconductor-to-metal transitions in monolayer $MoTe_2$. Our calculations showed that only a small fraction of 0.7% of the valence electrons has to be excited in order to tilt the balance towards the T' phase in the 14×14 supercell with 10% T' phase, which corresponds to $\approx 7\%$ of the T'-valence electrons, Figure 6(b,c). This is comparable to the 5% excited valence electrons reported by Kolobov et. al.[46] for $MoTe_2$, where the dynamical pathway was reconstructed using DFT molecular dynamics. Although our approach is by no means rigorous, it indicates that electronic excitations can also decrease the energy difference between the system with and without the T' phase island. The gain in energetics comes from the difference between the energy required to create an electron-hole pair in a semiconductor (band gap energy minus exciton binding energy) and a metal, which is essentially zero in the latter case. High power excitations (e.g. under laser irradiation) may even be sufficient to give rise to H to T transformations, but it is unlikely that electron beam in TEM under normal imaging conditions can alone give rise to the transformations.

Entropic contributions to the free energy at elevated temperatures. As the experiments were carried out at elevated temperatures, we also studied if entropic contributions can have noticeable effects on the thermodynamics of the system. The difference in the free energy of the T' and H

phases can be expressed as

$$\Delta F = F_{\mathrm{T'}} - F_{\mathrm{H}} = \Delta U - T\Delta S \tag{1}$$

where ΔU is the difference in the internal energy analyzed previously, and the entropy difference ΔS consists of two contribution; the vibrational entropy ΔS_{vib} and the electronic entropy ΔS_{elec}. Our DFT calculations of these contributions at a temperature of 1000 K revealed that both lower the energy difference between H phase and T' phase further facilitating the phase transition. The vibrational entropy difference between the pristine phases was evaluated to be $T\Delta S_{\mathrm{vib}} \sim 100$ meV/f.u. shifting the free energy balance towards the T' phase. The electronic entropy term is much smaller, and being of the order of $T\Delta S_{\mathrm{elec}} \sim 10$ meV/f.u. can essentially be neglected.

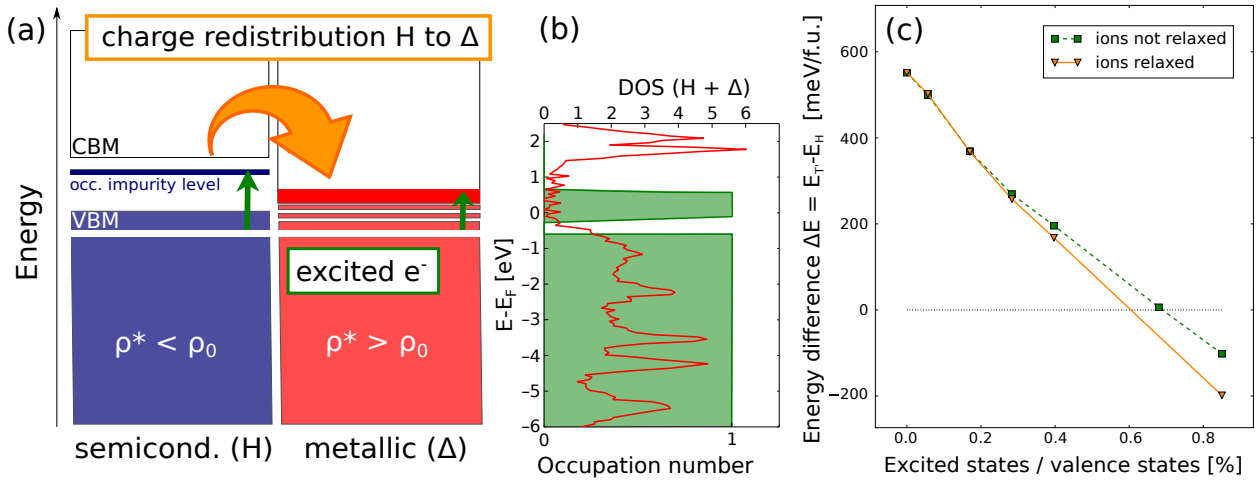

Figure 6: **Electronic excitations as a source for charge build-up.** (a) Schematic representation of the process. The microscope electron beam generates electronic excitations in the sample, with the excited electrons being localized in the T' phase island prior to their non-radiative recombination with holes. A quasi-stationary state forms as long as the sample is under the electron beam. (b) Electronic density of state of states of the system representing a T' phase island embedded into H matrix and the occupation numbers of the Kohn-Sham states used to mimic the effects of electron-beam-induced electronic excitations. (c) Energy difference between the metallic T' and the semiconducting H phases as a function of the excited states fraction with and without account for the relaxation of the positions of atoms.

The mechanism of local transformations from the H to T' phase induced by the electron beam. Our analysis indicates that none of the considered factors such as mechanical strain, vacancies, local charging, Re impurities, electronic excitations, or entropic contributions alone can explain

the local phase transitions observed in MoS_2 under electron beam irradiation.[5] However, our simulations indicate that all these factors lower the energy difference between the T' and H phases, so that their combination may be responsible for the observed transformation. One possible scenario favoring the metallic phase could involve the combination of $4-6\%$ local mechanical strain ($\Delta E_{\epsilon=4-6\%} \approx 150-250$ meV), $5-7\%$ Re impurities ($\Delta E_{\mathrm{Re}=5-7\%} \approx 150-250$ meV) and the effect of vibrational entropy $T\Delta S_{\mathrm{vib},T=1000K} \approx 100$ meV. On the other hand $4-5\%$ excitated valence electrons in the metallic region would suffice to tilt the balance towards T' phase ($\Delta E_{\mathrm{exc}} \approx 550-650$ meV).

Based on our results, we suggest the following scenario of the transformation: The electron beam creates vacancies through knock-on damage, beam-induced chemical etching and possibly electronic excitations.[47,48] The vacancies are highly mobile at elevated temperatures[49] and most of them cluster together into line defects.[32] Indeed, the alpha stripes discussed in Ref. 5 appear very similar to the vacancy lines. They naturally give rise to the development of mechanical strain in the MoS_2 flake, as a fraction of atoms in the system is lost. At the same time, the emerging vacancy lines are prerequisites for sulfur plane glides[5] to form the T' phase: S atoms cannot move to the hollow site positions in the H phase unless the neighboring S atoms are removed.[38] These factors, together with extra charge coming from Re impurities and quasi-stationary state involving electron excitation by primary high-energy electrons make the T' phase regions energetically favorable. Moreover, isolated vacancies still present in the system also decrease the energy difference between the phases. High temperature plays several roles. First, it facilitates vacancy agglomeration and makes it easier for the atoms to go over potential barriers, which is required for local atomic reconstructions. Second, it decreases the free energy difference between the phases mostly due to the changes in the vibrational degrees of freedom.

The created T' phase remains stable due to finite barriers between the configurations when the beam is switched off. Our results not only shed light on the mechanism of the beam-induced phase transitions observed in MoS_2, but also, with account for the variations in energy difference between the phases, are relevant to other 2D TMDs. The mechanism we discussed provides hints for further

developments and optimization of perhaps most intriguing aspects of 2D materials engineering using electron beam, as the seamless, nanoscale modification of the fundamental physical properties opens for device and circuit design with unparalleled combinations of miniaturization and integration. The possibilities are numerous, and since the phase-transformations are reversible through annealing, TMDs may be used in rewritable electronics. The understanding of the involved mechanisms is essential to develop rational routes to such extreme material modification using scalable techniques, such as for instance high brightness electron beam lithography.

Acknowledgements We thank Drs. K. Suenaga and M. Ghorbani-Asl for discussions. AVK acknowledges the Academy of Finland for the support under Project No. 286279, and the support from the U.S. Army RDECOM via contract No. W911NF-15-1-0606. The computational support from the HZDR computing cluster is gratefully appreciated. We also thank CSC-IT Center for Science Ltd. and Aalto Science-IT project for generous grants of computer time.

References

(1) Wang, Q. H.; Kalantar-Zadeh, K.; Kis, A.; Coleman, J. N.; Strano, M. S. Electronics and optoelectronics of two-dimensional transition metal dichalcogenides. *Nature Nanotech.* **2012**, *7*, 699–712.

(2) Chhowalla, M.; Shin, H. S.; Eda, G.; Li, L.-J.; Loh, K. P.; Zhang, H. The chemistry of two-dimensional layered transition metal dichalcogenide nanosheets. *Nature Chemistry* **2013**, *5*, 263–275.

(3) Qian, X.; Liu, J.; Fu, L.; Li, J. Quantum spin Hall effect in two-dimensional transition metal dichalcogenides. *Science* **2014**, *346*, 1344–1347.

(4) Choe, D.-H.; Sung, H.-J.; Chang, K. J. Understanding topological phase transition in monolayer transition metal dichalcogenides. *Phys. Rev. B* **2016**, *93*, 125109.

(5) Lin, Y.-C.; Dumcenco, D. O.; Huang, Y.-S.; Suenaga, K. Atomic mechanism of the

semiconducting-to-metallic phase transition in single-layered MoS_2. *Nature Nanotechnology* **2014**, *9*, 391–396.

(6) Kim, J. S.; Kim, J.; Zhao, J.; Kim, S.; Lee, J. H.; Jin, Y.; Choi, H.; Moon, B. H.; Bae, J. J.; Lee, Y. H.; Lim, S. C. Electrical Transport Properties of Polymorphic MoS_2. *ACS Nano* **2016**, *10*, 7500–7506.

(7) Kappera, R.; Voiry, D.; Yalcin, S. E.; Branch, B.; Gupta, G.; Mohite, A. D.; Chhowalla, M. Phase-engineered low-resistance contacts for ultrathin MoS_2 transistors. *Nature Materials* **2014**, *13*, 1128–1134.

(8) Cho, S.; Kim, S.; Kim, J. H.; Zhao, J.; Seok, J.; Keum, D. H.; Baik, J.; Choe, D.-H.; Chang, K. J.; Suenaga, K.; Kim, S. W.; Lee, Y. H.; Yang, H. Phase patterning for ohmic homojunction contact in $MoTe_2$. *Science* **2015**, *349*, 625–628.

(9) Nourbakhsh, A.; Zubair, A.; Sajjad, R. N.; Tavakkoli K. G., A.; Chen, W.; Fang, S.; Ling, X.; Kong, J.; Dresselhaus, M. S.; Kaxiras, E.; Berggren, K. K.; Antoniadis, D.; Palacios, T. MoS_2 Field-Effect Transistor with Sub-10 nm Channel Length. *Nano Letters* **2016**, acs.nanolett.6b03999.

(10) Zhang, C.; Kc, S.; Nie, Y.; Liang, C.; Vandenberghe, W. G.; Longo, R. C.; Zheng, Y.; Kong, F.; Hong, S.; Wallace, R. M.; Cho, K. Charge Mediated Reversible Metal-Insulator Transition in Monolayer $MoTe_2$ and $W_xMo_{1-x}Te_2$ Alloy. *ACS Nano* **2016**, *10*, 7370–7375.

(11) Shirodkar, S. N.; Waghmare, U. V. Emergence of Ferroelectricity at a Metal-Semiconductor Transition in a 1T Monolayer of MoS_2. *Phys. Rev. Lett.* **2014**, *112*, 157601.

(12) Rasmussen, F. A.; Thygesen, K. S. Computational 2D Materials Database: Electronic Structure of Transition-Metal Dichalcogenides and Oxides. *The Journal of Physical Chemistry C* **2015**, *119*, 13169–13183.

(13) Pandey, M.; Bothra, P.; Pati, S. K. Phase Transition of MoS_2 Bilayer Structures. *The Journal of Physical Chemistry C* **2016**, *120*, 3776–3780.

(14) Eda, G.; Yamaguchi, H.; Voiry, D.; Fujita, T.; Chen, M.; Chhowalla, M. Photoluminescence from Chemically Exfoliated MoS_2. *Nano Letters* **2011**, *11*, 5111–5116.

(15) Guo, Y.; Sun, D.; Ouyang, B.; Raja, A.; Song, J.; Heinz, T. F.; Brus, L. E. Probing the Dynamics of the Metallic-to-Semiconducting Structural Phase Transformation in MoS_2 Crystals. *Nano Letters* **2015**, *15*, 5081–5088, PMID: 26134736.

(16) Eda, G.; Fujita, T.; Yamaguchi, H.; Voiry, D.; Chen, M.; Chhowalla, M. Coherent Atomic and Electronic Heterostructures of Single-Layer MoS_2. *ACS Nano* **2012**, *6*, 7311–7317.

(17) Wang, L.; Xu, Z.; Wang, W.; Bai, X. Atomic Mechanism of Dynamic Electrochemical Lithiation Processes of MoS_2 Nanosheets. *Journal of the American Chemical Society* **2014**, *136*, 6693–6697, PMID: 24725137.

(18) Gao, P.; Wang, L.; Zhang, Y.; Huang, Y.; Liu, K. Atomic-Scale Probing of the Dynamics of Sodium Transport and Intercalation-Induced Phase Transformations in MoS_2. *ACS Nano* **2015**, *9*, 11296–11301.

(19) Chou, S. S.; Sai, N.; Lu, P.; Coker, E. N.; Liu, S.; Artyushkova, K.; Luk, T. S.; Kaehr, B.; Brinker, C. J. Understanding catalysis in a multiphasic two-dimensional transition metal dichalcogenide. *Nature Communications* **2015**, *6*, 8311.

(20) Fan, X.; Xu, P.; Zhou, D.; Sun, Y.; Li, Y. C.; Nguyen, M. A. T.; Terrones, M.; Mallouk, T. E. Fast and Efficient Preparation of Exfoliated 2H MoS_2 Nanosheets by Sonication-Assisted Lithium Intercalation and Infrared Laser-Induced 1T to 2H Phase Reversion. *Nano Letters* **2015**, *15*, 5956–5960, PMID: 26288218.

(21) Lee, S. C.; Benck, J. D.; Tsai, C.; Park, J.; Koh, A. L.; Abild-Pedersen, F.; Jaramillo, T. F.;

Sinclair, R. Chemical and Phase Evolution of Amorphous Molybdenum Sulfide Catalysts for Electrochemical Hydrogen Production. *ACS Nano* **2016**, *10*, 624–632, PMID: 26624225.

(22) Loh, T. A.; Chua, D. H. Origin of Hybrid 1T- and 2H-WS2 Ultrathin Layers by Pulsed Laser Deposition. *The Journal of Physical Chemistry C* **2015**, *119*, 27496–27504.

(23) Enyashin, A. N.; Yadgarov, L.; Houben, L.; Popov, I.; Weidenbach, M.; Tenne, R.; Bar-Sadan, M.; Seifert, G. New Route for Stabilization of 1T-WS_2 and MoS_2 Phases. *The Journal of Physical Chemistry C* **2011**, *115*, 24586–24591.

(24) Enyashin, A. N.; Seifert, G. Density-functional study of Li_xMoS_2 intercalates ($0 \leq x \leq 1$). *Computational and Theoretical Chemistry* **2012**, *999*, 13 – 20.

(25) Kan, M.; Wang, J. Y.; Li, X. W.; Zhang, S. H.; Li, Y. W.; Kawazoe, Y.; Sun, Q.; Jena, P. Structures and Phase Transition of a MoS_2 Monolayer. *The Journal of Physical Chemistry C* **2014**, *118*, 1515–1522.

(26) Nasr Esfahani, D.; Leenaerts, O.; Sahin, H.; Partoens, B.; Peeters, F. M. Structural Transitions in Monolayer MoS_2 by Lithium Adsorption. *The Journal of Physical Chemistry C* **2015**, *119*, 10602–10609.

(27) KC, S.; Zhang, C.; Hong, S.; Wallace, R. M.; Cho, K. Phase stability of transition metal dichalcogenide by competing ligand field stabilization and charge density wave. *2D Materials* **2015**, *2*, 035019.

(28) He, H.; Lu, P.; Wu, L.; Zhang, C.; Song, Y.; Guan, P.; Wang, S. Structural Properties and Phase Transition of Na Adsorption on Monolayer MoS_2. *Nanoscale Research Letters* **2016**, *11*, 1–8.

(29) Cheng, Y.; Nie, A.; Zhang, Q.; Gan, L.-Y.; Shahbazian-Yassar, R.; Schwingenschlogl, U. Origin of the Phase Transition in Lithiated Molybdenum Disulfide. *ACS Nano* **2014**, *8*, 11447–11453, PMID: 25375988.

(30) Cazaux, J. Correlations between ionization radiation damage and charging effects in transmission electron microscopy. *Ultramicroscopy* **1995**, *60*, 411–425.

(31) Wei, X.; Tang, D.-M.; Chen, Q.; Bando, Y.; Golberg, D. Local Coulomb explosion of boron nitride nanotubes under electron beam irradiation. *ACS nano* **2013**, *7*, 3491–7.

(32) Komsa, H.-P.; Kurasch, S.; Lehtinen, O.; Kaiser, U.; Krasheninnikov, A. V. From point to extended defects in two-dimensional MoS_2: Evolution of atomic structure under electron irradiation. *Physical Review B* **2013**, *88*, 035301.

(33) Kresse, G.; Hafner, J. Ab initio molecular dynamics for liquid metals. *Physical Review B* **1993**, *47*, 558–561.

(34) Kresse, G.; Furthmüller, J. Efficiency of ab-initio total energy calculations for metals and semiconductors using a plane-wave basis set. *Computational Materials Science* **1996**, *6*, 15–50.

(35) Perdew, J. P.; Burke, K.; Ernzerhof, M. Generalized Gradient Approximation Made Simple. *Physical Review Letters* **1996**, *77*, 3865–3868.

(36) Duerloo, K.-A. N.; Li, Y.; Reed, E. J. Structural phase transitions in two-dimensional Mo- and W-dichalcogenide monolayers. *Nature Communications* **2014**, *5*, 4214.

(37) Togo, A.; Oba, F.; Tanaka, I. First-principles calculations of the ferroelastic transition between rutile-type and $CaCl_2$-type SiO_2 at high pressures. *Phys. Rev. B* **2008**, *78*, 134106.

(38) Komsa, H.-P.; Krasheninnikov, A. V. Engineering the Electronic Properties of Two-Dimensional Transition Metal Dichalcogenides by Introducing Mirror Twin Boundaries. *Advanced Electronic Materials* **2017**, *0*, 1600468.

(39) Bertolazzi, S.; Brivio, J.; Kis, A. Stretching and breaking of ultrathin MoS_2. *ACS Nano* **2011**, *5*, 9703–9709.

(40) Lin, Y.-C.; Dumcenco, D. O.; Komsa, H.-P.; Niimi, Y.; Krasheninnikov, A. V.; Huang, Y.-S.; Suenaga, K. Properties of individual dopant atoms in single-layer MoS_2: atomic structure, migration, and enhanced reactivity. *Advanced materials* **2014**, *26*, 2857–61.

(41) Komsa, H.-P.; Krasheninnikov, A. V. Native Defects in Bulk and Monolayer MoS_2 from First Principles. *Phys. Rev. B* **2015**, *91*, 125304.

(42) Topsakal, M.; Ciraci, S. Effects of static charging and exfoliation of layered crystals. *Physical Review B* **2012**, *85*, 045121.

(43) Chan, K. T.; Lee, H.; Cohen, M. L. Possibility of transforming the electronic structure of one species of graphene adatoms into that of another by application of gate voltage: First-principles calculations. *Physical Review B* **2011**, *84*, 165419.

(44) Nozik, A. J. Spectroscopy and hot electron relaxation dynamics in semiconductor quantum wells and quantum dots. *Ann. Rev. Phys. Chem.* **2001**, *52*, 193–231.

(45) Kaasbjerg, K.; Thygesen, K. S.; Jacobsen, K. W. Phonon-limited mobility in n-type single-layer MoS_2 from first principles. *Phys. Rev. B* **2012**, *85*, 115317.

(46) Kolobov, A. V.; Fons, P.; Tominaga, J. Electronic excitation-induced semiconductor-to-metal transition in monolayer $MoTe_2$. *Physical Review B - Condensed Matter and Materials Physics* **2016**, *94*, 1–6.

(47) Krasheninnikov, A. V.; Banhart, F. Engineering of nanostructured carbon materials with electron or ion beams. *Nature Mater.* **2007**, *6*, 723–733.

(48) Krasheninnikov, A. V.; Nordlund, K. Ion and electron irradiation-induced effects in nanostructured materials. *J. Appl. Phys.* **2010**, *107*, 071301.

(49) Komsa, H.-P.; Kotakoski, J.; Kurasch, S.; Lehtinen, O.; Kaiser, U.; Krasheninnikov, A. V. Two-Dimensional Transition Metal Dichalcogenides under Electron Irradiation: Defect Production and Doping. *Phys. Rev.Lett.* **2012**, *109*, 035503.